ANL/CP--72944

DE92 001981

BOOTSTRAP AND FAST WAVE CURRENT DRIVE FOR TOKAMAK REACTORS*

D.A. Ehst
Fusion Power Program
Argonne National Laboratory
Argonne, IL 60439 USA

September 1991

* Work supported by the Office of Fusion Energy, U.S. Department of Energy under Contract Number W-31-109-Eng-38.

To be presented at the IAEA Technical Committee Meeting on Fast Wave Current Drive in Reactor Scale Tokamaks, Camargue, Arles, France, September 23-25, 1991.

BOOTSTRAP AND FAST WAVE CURRENT DRIVE FOR TOKAMAK REACTORS*

David A. Ehst
Argonne National Laboratory
Argonne, IL 60439 USA

ABSTRACT

Using the multi-species neoclassical treatment of Hirshman and Sigmar we study steady state bootstrap equilibria with seed currents provided by low frequency (ICRF) fast waves and with additional surface current density driven by lower hybrid waves. This study applies to reactor plasmas of arbitrary aspect ratio. In one limit the bootstrap component can supply nearly the total equilibrium current with minimal driving power (< 20 MW). However, for larger total currents considerable driving power is required (for ITER: I_o = 18 MA needs P_{FW} = 15 MW, P_{LH} = 75 MW). A computational survey of bootstrap fraction and current drive efficiency is presented.

1. INTRODUCTION

For many years plasma physics studies have pointed to the ion cyclotron range of frequencies (ICRF) as an attractive regime for high power radio wave applications. In addition to ion heating, direct electron heating has been a predicted capability; and the ability to generate non-thermal velocity distributions may offer additional opportunities to affect plasma behavior. The advent of high power experiments on large tokamaks has allowed some confirmation of these predicted results of ICRF techniques. Moreover, relative to neutral beams, ICRF technology is attractive for tokamak reactors for numerous reasons:

(a) the technology is mature
(b) the cost of injected power is low
(c) the transmission lines are readily shielded from neutron streaming
(d) the lines can contain tritium using windows
(e) the fast wave easily propagates into the high density plasmas desired for divertor plate protection
(f) tokamak and ICRF hardware maintenance is simplified with compact, reliable sources at a remote location
(g) plasma control may be greatly enhanced by rapid adjustments of frequency, power, and phase.

It is meet that we should now consider fast wave current drive (FWCD) as a further possibility with ICRF technology. We consider FWCD to be a natural extension of the ICRF capability for reactor-scale tokamaks, and for purpose of illustration we concentrate on the ITER design [1] in this paper.

* Work supported by the Office of Fusion Energy, U.S. Department of Energy under Contract No. W-31-109-Eng-38.

By itself FWCD is marginally acceptable for a commercial reactor due to physics limitations to the current drive efficiency. However, the bootstrap current [2] naturally adds to the central ("seed") current provided by FWCD, significantly amplifying the total current. In fact, the bootstrap current density may dominate the equilibrium, and its effect on the current profile must be calculated in order to accurately assess stability of the MHD equilibrium.

At some additional expense, more flexibility in current profile control might be achieved by adding a lower hybrid current drive (LHCD) system to a reactor, and we also consider this option. Unlike FWCD, the LHCD is limited by accessibility to the low pressure surface region of a tokamak. Separate control of the central and surface current density promises an exceptional potential for tailoring the MHD equilibrium. We will present surveys of steady-state equilibrium calculations and display a range of equilibria which might be produced. Our results in general have not been analyzed for stability, but the values of beta, safety factor, total current and internal inductance fall within the window of stability expected from other studies.

2. BOOTSTRAP MODEL

Bootstrap current density, which arises due to the radial gradients in density and temperature of a confined toroidal plasma, is a function on each flux surface, ψ, of electron and ion collisionality (ν_*), the local inverse aspect ratio (or magnetic well depth, ϵ), the ion species mixture, and the species' densities and temperatures, as well as their gradients. For axisymmetric tokamaks the relevant current density function is actually a flux surface average [3] $\langle j_\parallel B\rangle/\langle B^2\rangle = G(\psi) + H(\psi)$; in our notation $G(\psi)$ is the wave driven component and $H(\psi)$ is the bootstrap contribution, which we discuss in this section.

The complicated dependence of $H(\psi)$ on multiple independent variables makes it difficult to incorporate fully general but efficient computing algorithms in fast-running codes, so our treatment splices together simpler models in different regions of minor radius. In the hot interior of the plasma (where $\nu_* \leq 0.1$) we solve the Hirshman-Sigmar matrix equations [4] at arbitrary ϵ for the explicit ion mixture, however $H(\psi)$ is computed with $\nu_* \equiv 0$. On the other hand, in regions like the cold surface, where the plasma is in the Pfirsch-Schluter collision regime, the bootstrap transport coefficients are small and $H(\psi)$ is significantly reduced. Thus, at large collisionality ($\nu_* \geq 1.0$) we use the Hinton and Hazeltine [5] formulation of $H(\psi)$ with its explicit dependence on ν_*. This latter treatment assumes small ϵ and only treats multiple ions in an approximate fashion, but these inaccuracies are insignificant in those regions where $H(\psi)$ is itself small. Our code interpolates between these two formulations of $H(\psi)$ on flux surfaces with $0.1 \leq \nu_* \leq 1.0$.

As a check of our bootstrap calculations, an additional analytic expression, given by Hirshman [6], was studied. This formula treats the ions

as a single species and assumes $\nu_* \equiv 0$ but is valid at arbitrary ϵ. The results of using this formula are shown as the dashed curves in Figs. 1-2; we will find that this simple analytic expression agrees well with our matrix inversion of the Hirshman-Sigmar equations when all ions have the same temperature, provided the ion charge in Ref. 6 is replaced with $Z_{eff} = \sum(n_i/n_e)\, Z_i^2$.

In order to illustrate the effect of the plasma parameters on the bootstrap current we have studied the reference long pulse operating mode of the tokamak design [1] resulting from the ITER Conceptual Design Activity ("ITER/CDA"); see Table I. Our studies always assume a simple pressure profile, $p(\psi) = p_o\, \tilde{\psi}^{\alpha}$, where $\tilde{\psi}$ is normalized to unity at the magnetic axis, and the density and temperature are respectively parameterized as $n_j(\psi) = n_{jo}\, \tilde{\psi}^{e_n}$ and $T_j(\psi) = T_{jo}\, \tilde{\psi}^{e_T}$, where $e_n + e_T = \alpha$ and the exponents are the same for all species. Note that the bootstrap current is given in terms of gradients in ψ, not in real space gradients. In general $d/d\psi \neq 0$ at the magnetic axis. The objective of our present investigation is to compute the total bootstrap current, I_B, for given parameters. For a prescribed pressure, the diamagnetism $F(\psi) = RB_t$ is related to the parallel currents [3] as

$$\frac{1}{\mu}\frac{dF}{d\psi} + \frac{F}{\langle B^2\rangle}\frac{dp}{d\psi} = -\frac{G(\psi)}{2\pi} - \frac{H(\psi)}{2\pi} \quad . \tag{1}$$

The pressure and diamagnetism are further related by the Grad-Shafranov equation

$$j_t = -\frac{2\pi}{\mu R}\left[\, \mu R^2 \frac{dp}{d\psi} + F\frac{dF}{d\psi}\,\right] = \frac{R}{2\pi\mu}\,\nabla\cdot\left[\,\frac{\nabla\psi}{R^2}\,\right] \quad , \tag{2}$$

where j_t is the toroidal component of the current density. Except for corrections of order beta, the toroidal bootstrap current, found by substituting Eq. (1) into Eq. (2) and integrating j_t, is

$$I_B = \int_{\Delta\psi} d\psi\; q(\psi)\, F(\psi)\, H(\psi) \quad , \tag{3}$$

where $q(\psi)$ is the safety factor.

In the first study the total pressure was held constant while varying temperature and density. The density is typical of rather flat profiles, $e_n = 0.5$, and a pure deuterium plasma was selected. For ITER as the peak temperatures exceed ~10 keV it was found that the bootstrap current saturates ($I_B \simeq 7$ MA), the plasma being in the banana limit. This means a large bootstrap current results over a wide window of operating temperatures and densities.

Next the ion and electron temperatures were independently varied for a pure deuterium plasma. Since the electron density was held fixed at a volume average $\bar{n}_e = 1.06 \times 10^{20}$ m^{-3}, the varying temperatures had the effect of varying the poloidal beta, $\beta_I \equiv 2\mu\bar{p}/(\mu I_o/2\pi aS)^2$, where S is the shape factor and $\bar{p}$ is the volume-averaged pressure. As the bootstrap current is expected to be proportional to β_I [2], our calculated results are given in terms of the ratio I_B/β_I; see Fig. 1. These results, calculated with the same flat density ($e_n = 0.5$) profile, show that the bootstrap current is not very sensitive to the exact ratio T_e/T_i provided ITER operates with $T_{eo} \gtrsim 20$ keV and $T_{io} \gtrsim 20$ keV, as is likely. Note that the analytic expression for $H(\psi)$, the dashed curves, agrees rather well with the numerical matrix inversion solution, the open points. The qualitative behavior of I_B/β_I, a reduction as the ratio T_e/T_i decreases, can be understood by reference to the analytic expression [6].

The issue of impurity ion effects on neoclassical transport has always been an active concern, and an extensive survey of multiple-ion calculations of bootstrap current was performed, the results being summarized in Fig. 2. In this series the average electron density, $\bar{n}_e = 1.06 \times 10^{20}$ m^{-3}, and the density-weighted average temperatures, $\langle T_e \rangle_n = \langle T_i \rangle_n = 11.2$ keV, were held constant, but the total ion density varied in order to maintain quasineutrality, so the bootstrap current is again displayed normalized to β_I. The first observation to be made is that the simple analytic expression of Ref. 6 gives good accuracy provided Z_i is replaced with Z_{eff}. This is shown in the figure for: single ion plasmas, denoted by points labelled C, Be, and α (which is helium), as well as for pure Fe (not displayed); also for hydrogenic plasmas -- open circles -- which have less than a 1% difference between protons, deuterons, or tritons; also for a single ion minority, in parentheses, in deuterium; also for a typical ITER mixture, point a, of DT plus helium; and also for "advanced fuel" mixtures -- the square point -- of DHe^3 plus reaction products. It should be noted that all three curves in the figure turn over quickly for $Z_{eff} \gtrsim 10$, but the I_B/β_I values are probably already inaccurate at $Z_{eff} \approx 6$ because of our approximate treatment of collisionality. In any event, practical reactors will be restricted to the range $Z_{eff} \lesssim 3$.

These calculations were done for three different density gradients. For a given Z_{eff} it is seen that the most peaked density ($e_n = 1.0$) has the largest bootstrap current. However, even for extremely flat densities ($e_n = 0.05$) there is still a large bootstrap current, due to the compensating effect of the temperature gradient. A nonintuitive result is the increase in I_B/β_I with Z_{eff} for moderately flat density profiles, a behavior which is also evident upon close inspection of the analytic function for $H(Z_i)$ in Ref. 6.

Finally a series of runs was made with majority deuterium and a minority ion species at a different temperature. For these cases $T_{eo} \equiv 20$ keV and $n_{eo} = 1.7 \times 10^{20}$ m^{-3} ($\bar{n}_e = 1.06 \times 10^{20}$ m^{-3}). For deuterium with $T_{Do} = 20$ keV, a small amount of iron (~0.2%) was considered and T_{Feo} was varied. As seen in

Fig. 3 this resulted in only a minor effect on I_B/β_I. However, with ~10% helium in a deuterium majority, there was a significant variation with $T_{\alpha o}$. Moreover, reducing the helium to ~0.2% at $T_{\alpha o}$ = 1000 keV raised I_B/β_I again. Evidently, as the average ion temperature increases the normalized bootstrap current decreases, as might be expected from the trend displayed in Fig. 1 at constant T_e. An important limitation of our results is that the ions are taken to be thermal distributions in velocity; assigning an effective temperature to alpha particles, as in Fig. 3, may not properly model the bootstrap contribution of nonthermal species present in a reactor plasma.

3. SELECTION OF rf PARAMETERS FOR CURRENT DRIVE

The previous section demonstrated that approximately half of the total equilibrium current for ITER should arise from the bootstrap effect. We now determine the rf requirements needed to supply the remaining current density noninductively. In this and the following section we consider the nominal ITER/CDA steady state mode of operation with relatively high current and low density. This equilibrium has favorable stability characteristics, with a Troyon coefficient $g_T \approx 3.0$ % T • m/MA, provided the axis safety factor, q_a, is not far below unity, and provided $q(\psi)$ is monotonic and that the internal inductance is not too small. In addition to the parameters given in Table I, we limit our investigation to rather flat density (e_n = 0.5), and the ion mixture [1] is prescribed to yield Z_{eff} = 2.2. The fast alphas provide typically [1] about 20% of the plasma pressure, and they are modelled as a minority species at a high effective temperature (typically ~100-200 keV in this report). The fuel ions and impurities are at nearly the same temperature as the electrons.

The ITER/CDA provides an exceptional challenge to FWCD because the current I_o is large and the aspect ratio, A, is small. Our calculations of the rf current density, $G(\psi)$, use the normalized efficiency η from Ref. 7 in order to accurately calculate current driven in low A tokamaks in which magnetic trapping is detrimental. Using the RIP computer code we can trace ray trajectories of both fast and slow waves, and the absorbed power is calculated from linear damping on ions and electrons (the Landau as well as the transit-time-magnetic-pumping process).

Consider first LHCD, which offers the option of additional current density near the plasma surface in reactors. For ITER the generally agreed upon slow wave frequency [1] is f = 5.0 GHz. This is thought to be high enough to avoid the LHCD density cutoff [8] and is marginally high enough to avoid fusion alpha particle damping. Higher frequencies may be less attractive; at $f \gtrsim 5$ GHz the waveguide dimensions are small and the grill septa may be too thin for active cooling, except at the edges. Also, power generation and transmission efficiency tends to drop with increasing f. The appropriate parallel index of refraction, $n_\parallel$, for LHCD is determined by accessibility and Landau damping (LD). Our code computes linear damping, in order to speed execution, but the LHCD results -- wave penetration and

generated current -- have been shown to be in good agreement with more accurate quasilinear calculations [9].

There is some flexibility in choosing the launch location of the LH waves, so a survey of poloidal angles, θ, and $n_\parallel$ spectra was performed in order to find how to maximize wave penetration. The following results were found:

(a) accessibility is best (penetration to highest local n_e) for rays ending at the highest local magnetic field;
(b) penetration is best for outboard launch but varies little for $-0.2\pi \leq \theta \leq 0.2\pi$ (corresponding to ~1.3 m above or below the midplane in Fig. 4), varying from ~29% to 32% penetration in flux space;
(c) regardless of θ, the generated current, $G(\psi)$, is a maximum where LD is strongest, near the penetration limit for a given ray, and corresponds to normalized phase speeds $w \equiv \omega/k_\parallel v_e = 3.9\text{-}4.4$;
(d) the maximum of $G(\psi)$ and the penetration limit both occur in the vicinity of $T_e \sim 9.3\text{-}11.1$ keV;
(e) at maximum penetration the local well depth is $\varepsilon \simeq 0.21$ and the normalized efficiency, $\eta \simeq 11$, has been reduced by trapping effects to roughly 69% of the ideal value in a straight magnetic field [7].

Depending on θ, the minimum accessible $n_\parallel$ is ~1.8 for the profiles and parameters of the nominal steady state ITER/CDA. An important finding was that the resulting $G(\psi)$ from LHCD is fairly insensitive to θ, partly due to a negligible dependence of η on poloidal angle [7] for $w \gtrsim 2$. Thus, the actual location of the LHCD grill should probably be dictated by engineering criteria rather than physics concerns.

Turning next to FWCD, we find a variety of considerations play a role in choosing the wave parameters. Consider first the frequency. Experiments [8] on FWCD at high f ($\gtrsim$ 800 MHz) have generally exhibited a density limit, possibly due to spurious coupling to slow waves; however, at f $\lesssim$ 200 MHz the lower hybrid resonance density is so low that such deleterious coupling will not occur. Moreover, lower f reduces the cutoff density for a given $n_\parallel$ fast wave; for example, at f = 60 MHz there is essentially no evanescence in front of the antenna, the FW propagating at any $n_e > 3 \times 10^{17}$ m^{-3} when $n_\parallel = 2.0$. Likewise, accessibility to high density is possible even for $n_\parallel = 1.01$ as long as f $\lesssim$ 800 MHz. A possible issue [10] at low harmonics of the ion cyclotron frequency, $\omega/n\Omega_i < 1$, for $n \lesssim 6$, is coupling of FW power to ion Bernstein waves. This concern may be eliminated by selecting a low frequency which removes ion cyclotron resonances from the plasma.

The ray trajectories and radial absorption of fast waves on electrons also depend on f. In the inset in Fig. 4 the poloidal projection of rays with $n_\parallel = 2.0$ is shown, and the graph gives the resulting radial current density, $G(\psi)$, for these three frequencies. All three waves are absorbed in a

single pass through the plasma, but the lowest frequency (58 MHz) is clearly absorbed closest to the magnetic axis. At lower f ($\lesssim$ 20 MHz) wave absorption requires multiple passes (and ray tracing calculations become inaccurate).

In addition there are technological reasons for emphasizing rather low frequency for FWCD: source and overall system electric-to-rf efficiency may drop with frequency, so f $\lesssim$ 100 MHz would appear attractive. The final specification [1] for ITER, a tunable system with 15 MHz $\leq$ f $\leq$ 80 MHz, appears very attractive, allowing both ion heating and electron heating and FWCD either above or below the fundamental deuterium frequency. (It appears possible to avoid fast alpha damping even at f ~ 60 MHz by judicious design of the power spectrum, viz., $2 \lesssim n_{\parallel} \lesssim 5$. Our RIP calculation results at f ~ 60 MHz for FWCD are likely to be quite similar to results obtained at f ~ 20 MHz with a full-wave code.

The poloidal location of the ICRF antenna must be chosen with careful regard to the ion harmonic resonances. Even at A=2.8 it is possible to avoid strong ion damping. For example, as shown in Fig. 5, the $\omega = 2\Omega_T$ resonance can be located inboard of the magnetic axis, and $\omega = 2\Omega_D$ is at the outboard edge of the plasma, if f = 59 MHz. Those rays, all with $n_{\parallel} = 2.0$, started at $\theta = 0.4\,\pi$ and $0.3\,\pi$ suffer ~11% power lost to the tritium harmonic in a single pass, due to trajectories passing tangential to the $2\,\Omega_T$ surface, with no power loss to deuterium. A ray started at $\theta_o = 0.2\,\pi$ loses only ~6% of its power to ions. At $\theta = 0.1\,\pi$ about 10% of the power is lost, partly to the $2\Omega_D$ resonance; and at $\theta = 0.0$, nearly 79% of the power lost, mostly to harmonic deuterium. Ion damping can be made negligible for a single θ value by a slight adjustment of frequency; f = 62 MHz reduces ion absorption to 0.2% for $\theta = 0.4\pi$, while f = 58 MHz reduces ion absorption to 7% for $\theta = 0.0$.

It is also noteworthy in Fig. 5 for rays launched from $\theta \gtrsim 0.1\pi$ that substantial electron absorption occurs on the inboard side of a flux surface (the magnetic axis is 40 cm outboard of the geometric center). Such high field absorption minimizes the magnetic trapping reduction in η [7]. However, along a given ray path the maximum current generated occurs where w ~ 0.6-1.4, and for these low phase speeds trapping still results in a definite reduction in η. A typical example is the ray launched at $\theta_o = 0.3\,\pi$ for which $\eta = 5.7$ at the maximum of $G(\psi)$, at $\tilde{\psi} = 0.89$, where $\varepsilon = 0.094$; in a straight magnetic field the normalized current drive efficiency would be $\eta = 12.3$.

For each θ a series of $n_{\parallel}$ values was studied in order to identify the optimum spectrum for FWCD. It is generally the case that ion damping exceeds electron damping only for very small or very large $n_{\parallel}$. In the range $2.0 \lesssim n_{\parallel} \lesssim 3.0$, ion damping is less than 10% of the launched power, and less than ~4% of the wave's power remains after a single pass through the plasma. Results for FWCD are relatively insensitive to the exact $n_{\parallel}$ value in this range, so for the remaining calculations we have generally taken $n_{\parallel} = 2.0$. Finally, the limited poloidal extent of an ICRF antenna, typically about one meter, should result in a broad spectrum in the poloidal index of refraction,

and we attempt to simulate this in the RIP code by including several rays in the range $-2 \leq n_\theta \leq 2$ for each $n_\parallel$.

4. SELF-CONSISTENT rf DRIVEN EQUILIBRIA WITH BOOTSTRAP CURRENT

The RIP code iterates between solutions to Eqs. (1) and (2), starting with a given functional form for $F(\psi)$, computing the flux surface geometry $\psi(R,Z)$, tracing rays and determining the bootstrap terms in $G(\psi)$ and $H(\psi)$, and then updating $F(\psi)$ from the current density functions. Convergence occurs usually in about six to eight iterations, with $F(\psi)$ varying by <1% with subsequent iterations. We use typically two dozen rays and 100 spatial points in $\tilde{\psi}$.

The wave parameters can of course be selected to maximize the total current for a given rf input power. In addition, the wave parameters will determine the equilibrium current profile. Figure 6 illustrates a number of equilibria which all result from the same input power but with differing lower hybrid spectra. In each case the fast wave power, P_{FW}, is 15 MW, centered about $n_\parallel = 2.0$; the lower hybrid power, P_{LH}, is 75 MW, but the central $n_\parallel$ varies from 5.0 for the left hand column ($I_o = 17.4$ MA) to 2.1 at the right hand extreme ($I_o = 18.5$ MA). In each graph of $G(\psi)$ and $H(\psi)$ the solid curve is the initial equilibrium with the given $F(\psi)$, corresponding to the target value $I_o = 18.9$ MA, as in Table I. The chain-dotted curve is $H(\psi)$, and it is evident that the bootstrap current density is a large portion of the total desired. In fact, $I_B \simeq 12$ MA for all these equilibria. The function $G(\psi)$ is given by LHCD at the surface ($\tilde{\psi} \simeq 0$) and by FWCD ($\tilde{\psi} \simeq 1$); and the sum G + H is shown as a dotted curve. A number of observations should be made:

(a) at mid-minor radius, $\tilde{\psi} \simeq 0.5$, there is no contribution from wave driven currents;
(b) in all cases the converged solution (with $P_{FW} = 15$ MW plus $P_{LH} = 75$ MW) has I_o less than the desired value in Table I;
(c) despite the hollowness of the toroidal current density (for example, the case with $I_o = 17.4$) the safety factor $q(\psi)$ is not necessarily double valued;
(d) as the LHCD $n_\parallel$ is reduced, from left to right in the sequence of Fig. 6, the current increases, but $q(\psi)$ becomes nonmonotonic.

A limited number of converged equilibria were calculated for the ITER /CDA, with varying amounts of lower hybrid and fast wave power, and the resulting total currents are plotted in Fig. 7. It was usually possible to avoid double-valued $q(\psi)$ profiles, given large enough P_{FW}, but two results with nonmonotonic $q(\psi)$ are also included in the figure, as inverted triangles. Along each curve P_{LH} is held constant while P_{FW} varies, and the internal inductance increases with P_{FW}; we define the inductance as $\ell_i \equiv 2\,\overline{B_p^2}\,V\,[R_o/(\mu\,R_o\,I_o)^2]$, where V is the plasma volume. In one sense these results are appealing: the bootstrap current is typically ~60-70% of the total, which boosts the effective ("bootstrap aided") current drive figure

of merit as high as $\gamma_B \equiv \bar{n}_e R_o I_o/P_{CD} = 0.79$. On the other hand, it is disappointing that I_o is less than the required value (18.9 MA being desirable for good energy confinement), even with $P_{LH} = 75$ MW or $P_{CD} = 130$ MW.

5. EQUILIBRIUM AND PROFILE CONTROL AT HIGHER ASPECT RATIO

A more extensive survey of equilibria was done for the ITER high aspect ratio design ("ITER/HARD") option, at A = 4.0, as specified in Table I. We expect [2] the increase in β_I from the ITER/CDA to the ITER/HARD will offset the increase in A, so the bootstrap fraction, I_B/I_o will remain large. The larger A should modestly improve current drive efficiency (less magnetic trapping). However, the main improvement in this design is the lower I_o needed for confinement (albeit at a higher density).

Figure 8, a summary of the results, includes only solutions with monotonic $q(\psi)$. This figure is the focus of several observations. Note first that equilibria with $P_{LH} = 0$ are easily created. Eliminating the lower hybrid system is an attractive option for a reactor, as the hardware cost is relatively high and the electrical efficiency is low compared to the ICRF. In the limiting case we see equilibrium was found with a very minimal amount of rf power -- $I_o = 9.8$ MA with $P_{CD} = P_{FW} = 17.3$ MW. This case has $I_B/I_o = 0.90$, the highest bootstrap fraction we have found, and $\gamma_B = 3.64$. Despite the small input power $q(\psi)$ is monotonic and, at the axis, $q(0) = 1.8$. It is remarkable that nearly ten megamperes of (mostly bootstrap) toroidal current can be sustained with less than 20 MW of external power. Such low power input will minimize the heat load on the divertor plates of a reactor. The shortcoming of the bottom curve is that I_o is less than stipulated for confinement.

As in Fig. 7, an increase in P_{FW} at constant P_{LH} adds current density near the magnetic axis, increasing ℓ_i and reducing $q(\psi)$ near the axis. However, as seen from Eq. (3), this has the peculiar, unwanted effect of reducing I_B, since $q(\psi)$ appears in the integrand of that expression. Hence it is difficult to increase I_o for a fixed P_{LH} by adding fast wave power. In fact, the figure shows that I_o is mainly determined by P_{LH}, and the fast wave mostly controls the profile shape near the magnetic axis.

Thus, in order to achieve $I_o \geq 11.7$ MA, as specified for ITER/HARD confinement, $P_{LH} \approx 50$ MW is needed. We found that the minimum power needed for equilibrium with $I_o = 11.9$ MA is $P_{LH} = 56.4$ MW and $P_{FW} = 19.5$ MW. This special case is shown in Fig. 9 along with the ray trajectories. The ICRF antenna spans a distance ~1.5 m above the midplane, which appears to be an acceptable location in a reactor. The MHD and plasma parameters closely match the target values in Table I. The bootstrap fraction is $I_B/I_o = 0.75$, and $q(0) = 2.0$. The inductance, $\ell_i = 0.45$, is, however, rather low.

Reactor design criteria for the ITER/HARD are still under discussion, but three simultaneous constraints have been proposed for this nominal steady state: $I_o \geq 11.7$ MA; $P_{CD} \leq 113$ MW; and $\ell_i \geq 0.75$. Reference to Fig. 8 shows

that any combination of two of these three constraints can be satisfied, but all three can not be achieved together. The true requirement on ℓ_i will depend on detailed stability studies, which have not yet been done for these ITER equilibria with FWCD. We note, however, that similar FWCD results were tested and found stable to ideal modes [11] for the ARIES reactor study. An appealing aspect of FWCD is the ability to control $q(\psi)$, for, unlike inductive discharges, $q(0) \simeq 2.0$ is easily obtained (see Fig. 9); operation in this fashion might achieve "second stability".

6. CONCLUSIONS

If FWCD provides current density near the magnetic axis it will support a bootstrap current which can comprise a large fraction of the total equilibrium current, even with rather flat density profiles. At low total current very little rf power (< 20 MW) is needed. If, however, very large current is needed, then considerable LHCD and FWCD power is needed (~ 100 MW), and the current and safety factor profiles can be controlled by adjusting the ratio P_{LH}/P_{FW}. Thus, in addition to heating to ignition, it appears likely that the fast wave may offer valuable opportunities to enhance the performance of tokamak reactors.

ACKNOWLEDGMENT

I thank D. Pearlstein for his assistance in calculating the bootstrap current.

REFERENCES

[1] ITER Conceptual Design Report, ITER Documentation Series No. 18, IAEA, Vienna (1991).
[2] HSIAO, M.-Y., EHST, D.A., EVANS, JR., K., Nucl. Fusion **29** (1989) 49.
[3] EHST, D.A., Nucl. Fusion **25** (1985) 629.
[4] HIRSHMAN, S.P. SIGMAR, D.J., Nucl. Fusion **21** (1981) 1079.
[5] HINTON, F.L., HAZELTINE, R.D., Rev. Mod. Phys. **48** (1976) 239.
[6] HIRSHMAN, S.P., Phys. Fluids **31** (1988) 3150.
[7] EHST, D.A., KARNEY, C.F.F., Nucl. Fusion **31** (1991) to be pub.
[8] EHST, D.A., "Fast Wave Current Drive: Experimental Status and Reactor Prospects," Argonne National Laboratory ANL/FPP/TM-219 (1988).
[9] "TIBER II/ETR Final Design Report," Lawrence Livermore National Laboratory UCID-21150 (1987), Vol. 1, Appendix 2.B.
[10] CHIU, S.C., et al., Nucl. Fusion **29** (1989) 2175.
[11] EHST, D.A., EVANS, JR., K., KLASKY, M., Phys. Rev. Lett. 64 (1990) 1891.

Table I
ITER Parameters for Current Drive Studies

Parameter	Symbol	Units	ITER/CDA Long Pulse (Hybrid)	ITER/CDA Nominal Steady State	ITER/HARD Steady State
major radius	R_o	m	6.0	6.0	6.0
aspect ratio	A		2.8	2.8	4.0
elongation	κ		2.0	2.0	2.1
triangularity	d		0.55	0.55	0.55
vacuum field	B_o	T	4.85	4.85	7.00
pressure exponent	α		1.5	1.5	1.5
beta	β_t	%	4.0*	5.2	3.2
total current	I_o	MA	15.4	18.9	11.7
poloidal beta	β_I		1.11*	1.12	1.63
electron density	$\bar{n}_e$	$10^{20}m^{-3}$	1.06*	0.64	1.07
electron temperature	$\langle T_e \rangle_n$	keV	11*	20	17
density exponent	e_n		0.5*	0.5	0.5

* Standard case for bootstrap studies.

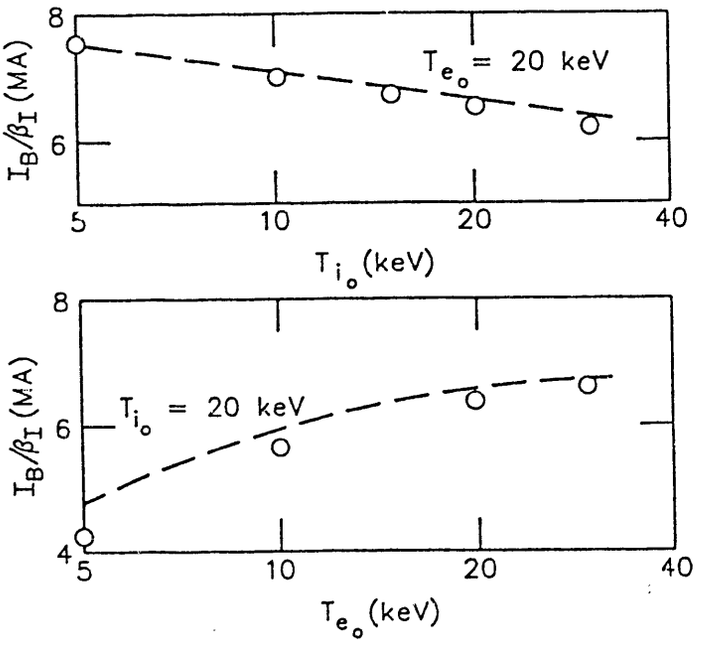

Fig. 1 Bootstrap current with unequal ion and electron temperatures, pure deuterium.

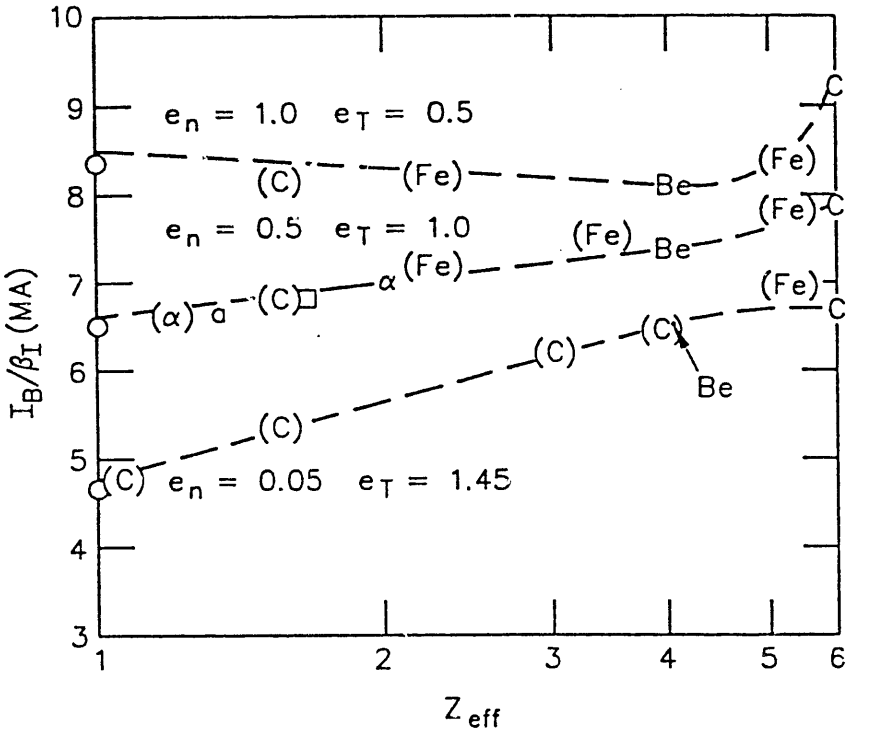

Fig. 2 Bootstrap current for different density and temperature profiles and various ion mixtures; $\bar{n}_e = 1.1 \times 10^{20}$ m^{-3}, $\langle T_e \rangle = \langle T_i \rangle = 11$ keV.

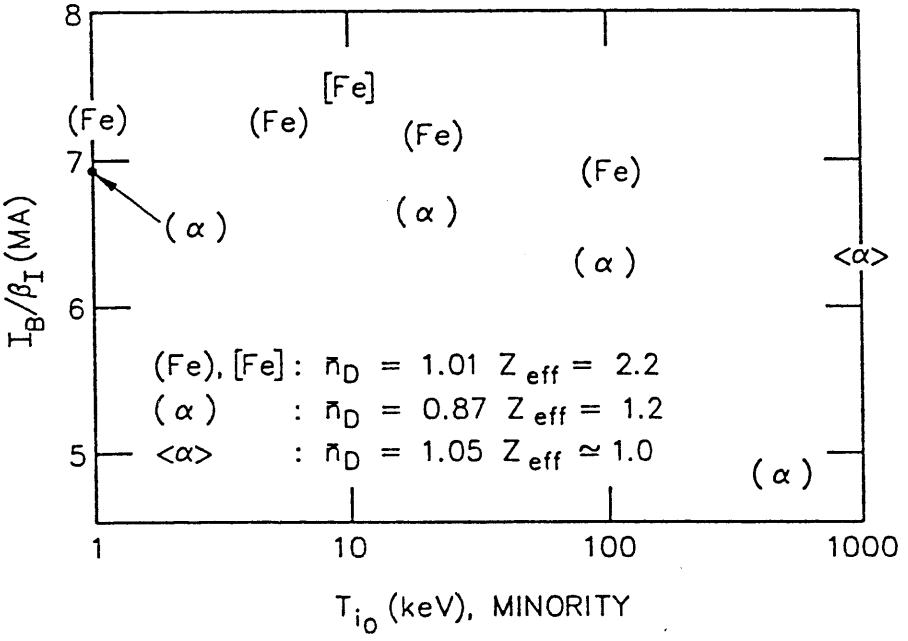

Fig. 3 Bootstrap current with unequal majority and minority ion temperatures. Deuterium at 20 keV peak, except for [Fe] at 10 keV peak.

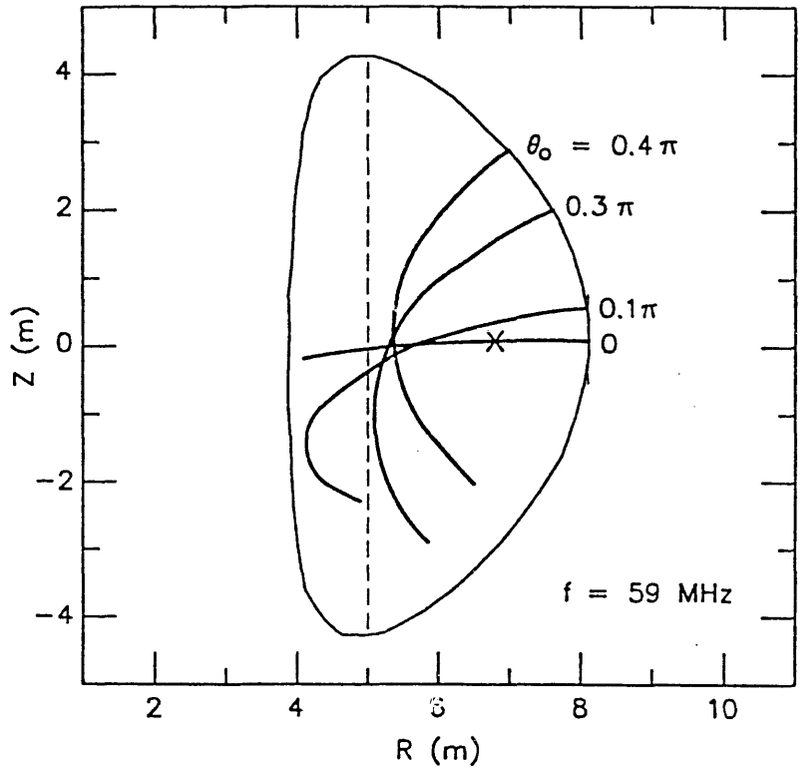

Fig. 5 Ray trajectories for various starting locations; second tritium harmonic on high field side of magnetic axis and second deuterium harmonic at outboard edge.

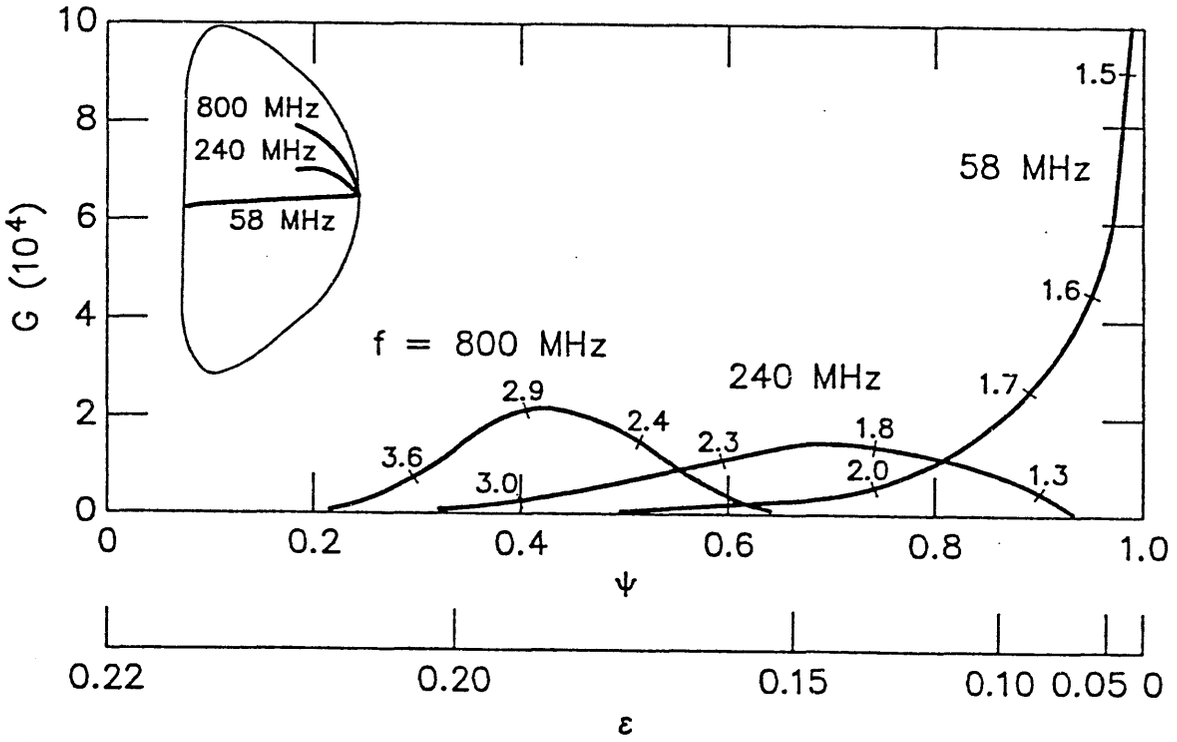

Fig. 4 Ray trajectories and radial current profiles for different fast wave frequencies; phase speed is indicated along G curves.

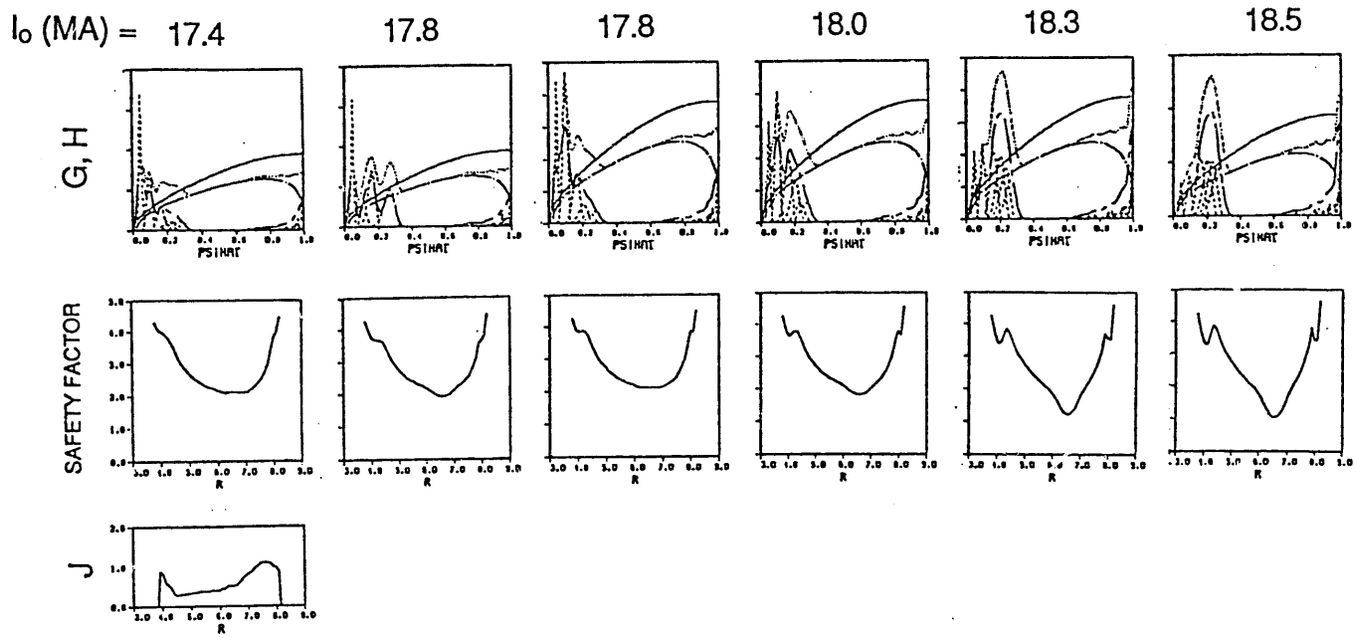

Fig. 6 Equilibria with bootstrap current and P_{LH} = 75 MW plus P_{FW} = 15 MW but different wave spectra; current and safety factor can be varied. (Vertical scale is not uniform for G and H.)

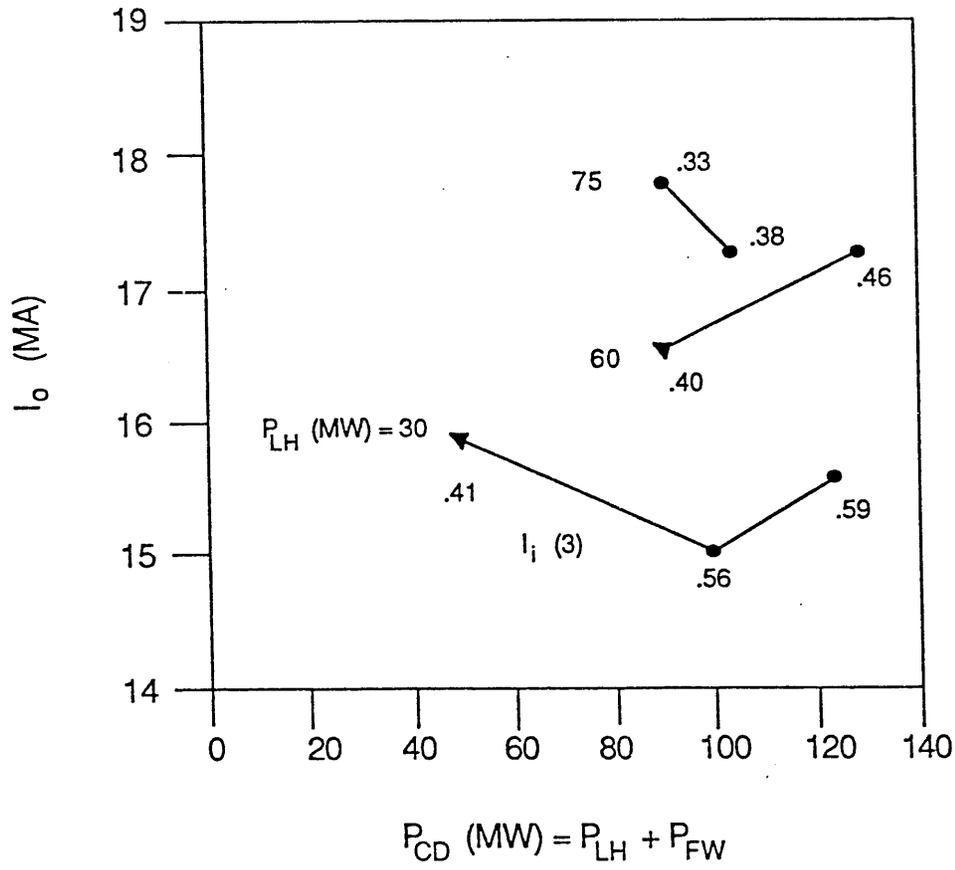

Fig. 7 Total current vs. lower hybrid and fast wave power; ITER/CDA at A = 2.8, $\bar{n}_e = 0.6 \times 10^{20}$ m^{-3}. Internal inductance is indicated.

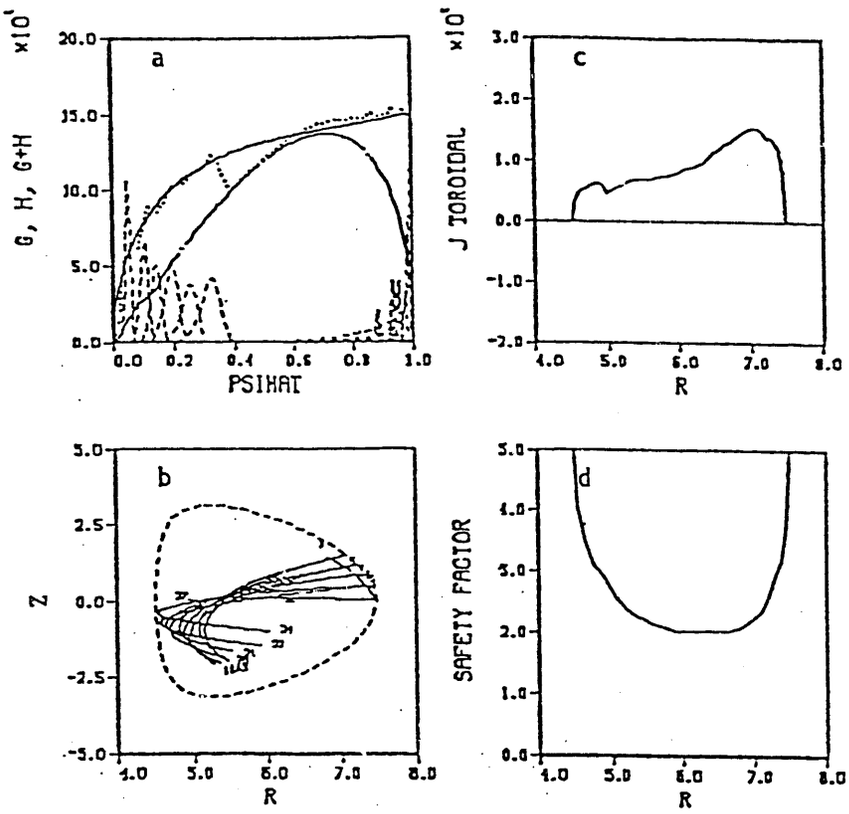

Fig. 9 Equilibrium at $\bar{n}_e$ = 1.1 x 10^{20} m^{-3}, A = 4.0, I_o = 11.9 MA, beta = 3.4%, with P_{CD} = 76 MW: a) currents vs. minor radius, b) ray paths, c) toroidal component of current across midplane, d) safety factor. Internal inductance is 0.45.

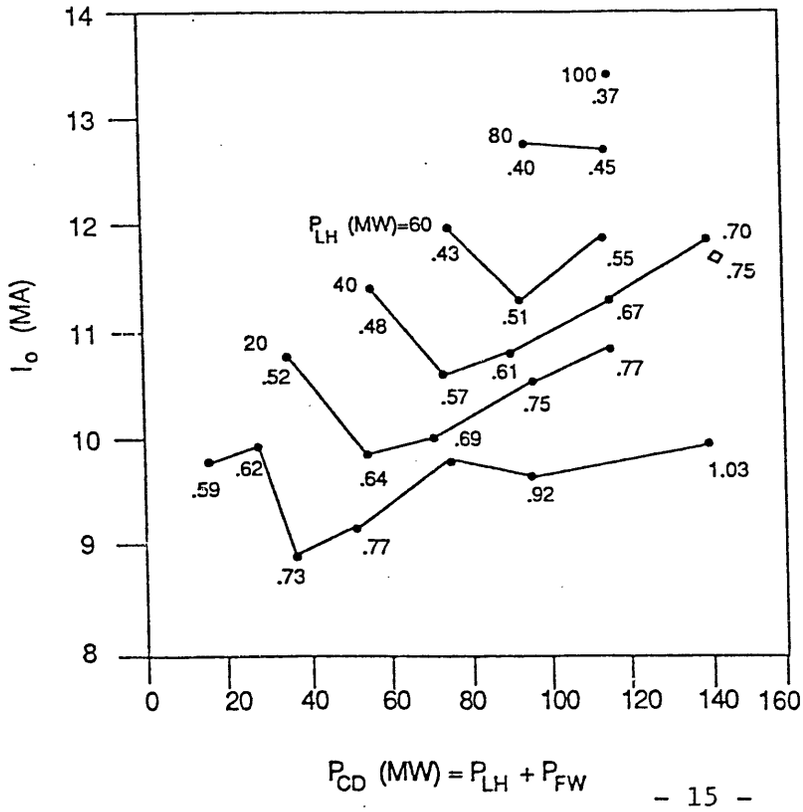

Fig. 8 Lower hybrid and fast wave power for steady state current drive with bootstrap current included; ITER/HARD: A=4.0, R_o=6.0 m, B_o=7.0 T, $\tilde{n}_e$ = 1.0 x 10^{20} m^{-3}, $\langle T_e \rangle$ = 16 keV. Diamond has P_{LH} = 35 MW.

END

DATE FILMED

12/06/91